THE JOURNAL OF BIOLOGICAL CHEMISTRY
Vol. 276, No. 42, Issue of October 19, pp. 39150–39160, 2001

Printed in U.S.A.

The Coatomer-interacting Protein Dsl1p Is Required for Golgi-to-Endoplasmic Reticulum Retrieval in Yeast*

Received for publication, June 22, 2001, and in revised form, August 6, 2001
Published, JBC Papers in Press, August 7, 2001, DOI 10.1074/jbc.M105833200

Uwe Andag, Tanja Neumann, and Hans Dieter Schmitt‡

From the Department of Molecular Genetics, Max-Planck-Institute for Biophysical Chemistry, D-37070 Göttingen, Germany

Sec22p is an endoplasmic reticulum (ER)-Golgi v-SNARE protein whose retrieval from the Golgi compartment to the endoplasmic reticulum (ER) is mediated by COPI vesicles. Whether Sec22p exhibits its primary role at the ER or the Golgi apparatus is still a matter of debate. To determine the role of Sec22p in intracellular transport more precisely, we performed a synthetic lethality screen. We isolated mutant yeast strains in which *SEC22* gene function, which in a wild type strain background is non-essential for cell viability, has become essential. In this way a novel temperature-sensitive mutant allele, *dsl1-22*, of the essential gene *DSL1* was obtained. The *dsl1-22* mutation causes severe defects in Golgi-to-ER retrieval of ER-resident SNARE proteins and integral membrane proteins harboring a C-terminal KK*XX* retrieval motif, as well as of the soluble ER protein BiP/Kar2p, which utilizes the HDEL receptor, Erd2p, for its recycling to the ER. *DSL1* interacts genetically with mutations that affect components of the Golgi-to-ER recycling machinery, namely *sec20-1*, *tip20-5*, and COPI-encoding genes. Furthermore, we demonstrate that Dsl1p is a peripheral membrane protein, which *in vitro* specifically binds to coatomer, the major component of the protein coat of COPI vesicles.

Membrane-bound compartments in eukaryotic cells can fuse directly as shown for the endoplasmic reticulum (ER)[1] and mitotic Golgi fragments as well as endosomal and lysosomal compartments (homotypic fusion; see Ref. 1). However, vectorial transport between distinct compartments mainly involves small coated vesicles whose formation from the donor membrane is mediated by proteinaceous coats, either COPI, COPII, or clathrin. After uncoating, vesicles fuse selectively with an acceptor membrane (heterotypic fusion; see Ref. 2). Both homotypic and heterotypic fusion events rely on specific attachment reactions to guarantee that only appropriate membranes can mix. The membrane attachment itself consists of two steps, tethering and docking, involving different sets of proteins (3, 4). Tethering factors are peripherally membrane-associated protein complexes consisting of up to 10 different subunits, which share little sequence similarity.

The subsequent docking stage involves specific sets of membrane-anchored proteins, so-called SNARE proteins (SNARE is soluble NSF (for *N*-ethylmaleimide-sensitive fusion protein) attachment protein receptor) (5–7). SNAREs are inserted into the membrane either by a C-terminal transmembrane domain or through lipid moieties attached to C-terminal cysteine residues. In contrast to the tethering factors, all known SNARE proteins are members of either of three protein families: the syntaxins, the synaptobrevins or VAMPs, and the SNAP-25 family members. To induce membrane fusion, SNARE proteins from apposed membranes must interact in *trans*. The formation of a stable four-helix bundle may generate enough energy to promote mixing of the lipid bilayer (8–10).

Lipid mixing experiments using SNARE complexes reconstituted into lipid bilayer vesicles indicated that only cognate SNARE combinations are able to induce fusion (11). However, SNARE proteins are rather promiscuous when the formation of the tight SDS or heat-resistant SNARE complexes is analyzed (12, 13). Moreover, SNARE proteins can be part of more than one SNARE complex *in vivo* (14), and some SNARE proteins can functionally replace each other (15, 16). *In vitro* the synaptobrevin/VAMP homologs Snc1p and Snc2p in yeast can be replaced by two other members of the synaptobrevin family, the ER-Golgi SNARE Sec22p and the vacuolar SNARE Nyv1p (11). However, these SNAREs are unable to replace Snc1/2p *in vivo* (17), probably because they are retained in their specific compartments. Thus, the targeting of SNAREs to the right compartment is one way to increase the specificity of intracellular membrane attachment/fusion events.

We analyzed previously (18) the targeting of the ER-to-Golgi SNARE Sec22p and show that the correct targeting of Sec22p involves its recycling from the Golgi to the ER via COPI-coated vesicles. In this respect, Sec22p as well as Bos1p (19) behave like ER-resident proteins that carry a KK*XX* ER-retrieval signal (20). The coat of COPI vesicles in mammalian cells and yeast consists of seven subunits (α-, β-, β'-, γ-, δ-, ϵ-, and ζ-COP) and the small GTPase, ARF1 (21).

The observations made by Letourneur *et al.* (20) and Cosson *et al.* (22) that KK*XX*-tagged proteins require COPI components for retrieval from Golgi to the ER provided first evidence that COPI vesicles mediate this retrograde transport. The same is true not only for Sec22p but also for other yeast proteins that recycle from Golgi to ER, for example, Emp47p, a Golgi lectin-like protein; Erd2p, the HDEL receptor; Sed5p, a Golgi-localized syntaxin homolog; and Mnn1p, a glycosyltransferase (23–26). How Sec22p is sorted into COPI vesicles is currently unknown. Moreover, the function of Sec22p is not entirely understood. The *SEC22* gene was first isolated by us as a multicopy suppressor of defects in the small GTPase Ypt1p

* This work was supported by Deutsche Forschungsgemeinschaft Grant SFB523. The costs of publication of this article were defrayed in part by the payment of page charges. This article must therefore be hereby marked "*advertisement*" in accordance with 18 U.S.C. Section 1734 solely to indicate this fact.

‡ To whom correspondence should be addressed. Tel.: 49-551-201-1713; Fax.: 49-551-201-1718; E-mail: hschmit@gwdg.de.

[1] The abbreviations used are: ER, endoplasmic reticulum; HDEL, C-terminal motif of histidine-aspartate-glutamate-leucine; α, α-factor pheromone; COP, coat protein; DAPI, 4′,6-diamidino-2-phenylindole; GFP, green fluorescent protein; GST, glutathione *S*-transferase; SDS-PAGE, sodium dodecyl sulfate polyacrylamide gel electrophoresis; Sec22-α, α-factor-tagged Sec22 protein; SNARE, receptor for SNAPs; Ts$^-$ mutant, temperature-sensitive mutant; ORF, open reading frame; 5-FOA, 5-fluoroorotic acid; PDI, protein disulfide isomerase.

TABLE I
Yeast strains

Strain	Genotype	Source
BSH-7C	*MATα, ura3, trp1, his3, suc2-Δ9, bet1-1*	This laboratory
MLY-100	*MATα, ura3, ade2, trp1, ufe1*::*TRP1,* containing pUFE315 (*UFE1*)	M. Lewis
MLY-101	*MATα, ura3, ade2, trp1, ufe1*::*TRP1,* containing pUT1 (*ufe1-1*)	M. Lewis
MSUC-2D	*MATα, ura3, leu2, his3*	This laboratory
MSUC-3B	*MATa, ade2, ura3, leu2, his3*	This laboratory
MSUC-7C	*MATα, ade8, ura3, leu2, his3*	This laboratory
PC70	*MAT*a, *ura3, leu2, trp1, ret1-1*	P. Cosson
PC82	*Mata, ura3, leu2, his3, lys2, ste2*::*LEU2, STE2-WBP1*::*URA3, sec21-2*	P. Cosson
PC137	*MAT*a, *ura3, leu2, his4, trp1, lys2, suc2-Δ9, tip20-5*	P. Cosson
RH236-3A	*MATα, ura3, leu2, his4, sec20-1*	H. Riezman
RH239-5A	*MATα, ura3, his4, leu2, lys2, sec21-1*	H. Riezman
RH270-2B	*MAT*a, *ura3, leu2, his4, lys2, bar1-1*	H. Riezman
SC23-3A	*MATα, leu2, ura3, his3, trp1, lys2, ade8, suc2-Δ9, sec23-1*	This laboratory
SHC22-12A	*MATα, ura3, his3, lys2, suc2-Δ9, sec22-3*	This laboratory
SL1-2B	*MATα, leu2, ura3, lys2, suc2-Δ9, sly1*^{ts}	This laboratory
SLA28-6C	*MATα, ade2, ade8, ura3, leu2, his3, trp1, sec22*::*HIS3* containing pHDS228 (*CEN6/ARS4, URA3, ADE8, SEC22*)	This laboratory
STE2-4B	*MATa, ura3, leu2, his3, lys2, ste2*::*LEU2, STE2-WBP1*::*URA3, bar1-1*	This laboratory
S20P4/3-9A	*MATα, ura3, leu2, lys2, pep4*::*HIS3, sec20-1*	This laboratory
S21P4-9A	*MAT*a, *leu2, ura3, pep4*::*HIS3, sec21-1*	This laboratory
S27P4-9C	*MATα, leu2, ura3, lys2, pep4*::*HIS3, sec27-1*	This laboratory
S32G-8A	*MATα, ura3, leu2, his3, sec32-1/bos1*	This laboratory
SUA1-3D	*MATα, ade2, ade8, ura3, leu2, his3, trp1, sec22*::*HIS3*	This study
SUA1-12D	*MAT*a, *ade2, ade8, ura3, leu2, his3, lys2, sec22*::*HIS3* containing pHDS228 (*CEN6/ARS4, URA3, ADE8, SEC22*)	This study
SUA5	*MATa, ura3, leu2, his3, lys2, ste2*::*LEU2, STE2-WBP1*::*URA3, bar1-1, dsl1-22-6His-2myc*::*loxP-Kan*MX-*loxP*	This study
TNY51	*MATα, ura3, leu2, his3, trp1, lys2, ade2, sed5-1*	This laboratory
TNY140	*MAT*a, *leu2, ura3, lys2, his4, sec27-1*	This laboratory
Y21186	*MATa/α, ura3Δ0/ura3Δ0, leu2Δ0/leu2Δ0, his3Δ1/his3Δ1, lys2Δ0/LYS2, MET15/met15Δ0, YNL258c*::*Kan*MX/*YNL258c*	Euroscarf
YUA1-9C	*MATα, ade2, ura3, leu2, his3, lys2, dsl1-22*	This study
YUA3-1A	*MATα, ade2, ura3, leu2, his3, pep4*::*HIS3*	This study
YUA3-4B	*MATα, ade2, ade8, ura3, leu2, his3, pep4*::*HIS3, dsl1-22*	This study
YUA11	*MAT*a, *ura3, leu2, his4, lys2, bar1-1, DSL1-6His-2myc*::*loxP-Kan*MX-*loxP*	This study
YUA41	*MAT*a, *ura3, leu2, his4, lys2, bar1-1, dsl1-22-6His-2myc*::*loxP-Kan*MX-*loxP*	This study

involved in ER-to-Golgi transport (named *SLY2*; see Ref. 27). Later *SLY2* was found to be identical to *SEC22* (28) for which conditional mutant alleles had been identified by Novick *et al.* (29). Like several other SNARE proteins, Sec22p can be a component of more than just one SNARE complex. Its physical interaction with the SNARE proteins Sed5p, Bos1p, Bet1p, and other Golgi SNARE proteins argues for a role in anterograde traffic from ER-to-Golgi (6, 30, 31). Sec22p also co-precipitates with the ER proteins Ufe1p and Sec20p that function in retrograde Golgi-ER transport (24, 32, 33). *sec22* mutants lead to a defect in forward traffic (34–37). However, this defect, as with many other mutants affected in retrograde transport, could be a secondary effect. *In vitro* assays performed with permeabilized mutant cells showed that the *sec22-3* mutation does not slow down forward transport but does inhibit retrograde transport (38, 39). Membrane fusion reconstituted with liposomes containing the ER-to-Golgi SNARE Bet1p requires the presence of Sec22p along with Sed5p and Bos1p on the opposing membranes to drive fusion (11, 40). In mammalian cells the Sec22p homolog sec22b coprecipitates with syntaxin 5 (~Sed5p), rbet1 (~Bet1p), and membrin (~Bos1p) (41) as well as syntaxin 18, which may be functionally equivalent to Ufe1p (42). Therefore, the dual function of Sec22p may be conserved throughout evolution.

To obtain additional clues to the function of Sec22p, we used a genetic approach. *SEC22* is not essential for cell viability (27). We tried to find mutant yeast strains in which *SEC22* became essential. A new allele of yeast ORF *YNL258c* showed synthetic lethality with *sec22*Δ. Mutants in *YNL258c* were recently shown to be dependent on a dominant allele of *SLY1,* a suppressor of many ER-to-Golgi transport defects, and the gene was named *DSL1* (43). Evidence was provided for a function of Dsl1p in ER-to-Golgi forward transport. Genetic interaction of some *dsl1* mutants with the γ-COP-encoding *SEC21* gene also suggested a role of Dsl1p in retrograde Golgi-to-ER traffic (43). We show that a new allele of *DSL1*, *dsl1-22,* isolated in our screen indeed affects Golgi-to-ER retrieval of several proteins with only slight effects on forward transport. *dsl1-22* interacts genetically with factors required for retrograde traffic, and Dsl1p binds coatomer. Taken together, our data provide strong evidence for a direct role of Dsl1p in Golgi-to-ER traffic.

EXPERIMENTAL PROCEDURES

Yeast Strains, Genetic Techniques, and Plasmids—Saccharomyces cerevisiae strains used are listed in Table I. Cells were grown in yeast extract/peptone/dextrose or synthetic minimal medium containing galactose (2%) or glucose (2%) as carbon sources and supplemented as necessary with 20 mg/liter tryptophan, histidine, adenine, uracil or 30 mg/liter leucine or lysine. To enhance the visualization of sectoring colonies, plates with low adenine concentration (10 mg/liter adenine) were prepared. 5-FOA plates were prepared as synthetic minimal medium containing 0.1% 5-FOA. Yeast transformations were performed as described previously (44). Standard techniques were used for mating of haploid strains, complementation analysis, sporulation, and the analysis of tetrads (45). The assay to detect retention defects using Ste2-Wbp1p was described previously (20, 46). The analysis of synthetic lethal effects between the *dsl1-22* mutation and other ER-Golgi defects was performed with strains derived from the original mutant by three crosses to wild type strains or a *dsl1-22-myc*::*Kan*MX strain derived from the original transformant by two crosses to wild type strains. When possible tetrad analysis was performed 2 or 3 days after placing diploid cells on potassium acetate plates. The viability of spores varied considerably. Therefore, the genotype of viable spores was determined by crosses to tester strains (complementation assays). The *dsl1-22-myc*::*Kan*MX carrying spores were identified by their resistance to G418. 98% of the possible *dsl1-22*, *sec23-1*, mutants, 80% of the possible *dsl1-22, bet1-1* double mutants, 64% of the *dsl1-22, sec27-1*, 47% of the *dsl1-22, sec22-3,* 36% of the *dsl1-22,*

TABLE II
Plasmids

Plasmid name	Description	Source
pHDS228	pRS316-*SEC22-ADE8, URA3, CEN6/ARS4*	This laboratory
pPR177	pGEX-TT-*TIP20*	R. Peng
pTN159	pUG36-*SEC22, URA3, CEN6/ARS4*	This study
pUA18	pRS315-*sec22-3, LEU2, CEN6/ARS4*	This study
pUA20	pRS315-*SEC22, LEU2, CEN6/ARS4*	This study
pUA26	pGEX-TT-*SEC22*Δ*c*	This study
pUA30	pGEX-TT-*BOS1*Δ*c*	This study
pUA37	pRS315-*BOS1, LEU2, CEN6/ARS4*	This study
pUA39	pRS315-*UFE1, LEU2, CEN6/ARS4*	This study
pUA40	pRS315-*SED5, LEU2, CEN6/ARS4*	This study
pUA42	pGEX-TT-*SED5*Δ*c*	This laboratory
pUA43	pRS325-*SED5, LEU2, 2*μ*m*	This study
pUA44	pRS325-*UFE1, LEU2, 2*μ*m*	This study
pUA45	pRS325-*BOS1, LEU2, 2*μ*m*	This study
pUA65	pRS315-*YKT6, LEU2, CEN6/ARS4*	This study
pUA73	pRS315-*DSL1, LEU2, CEN6/ARS4*	This study
pUA74	pRS315-*YNL260c, LEU2, CEN6/ARS4*	This study
pUA81	pRS325-*DSL1, LEU2, 2*μ*m*	This study
pUA86	pRS315-*dsl1-22, LEU2, CEN6/ARS4*	This study
pUA87	pRS315-*YNL258c-ATX1-YNL260c, LEU2, CEN6/ARS4*	This study
pUA93	pGEX-TT-*DSL1*	This study
pUA94	pGEX-TT-*dsl1-22*	This study
pUA101	pEG-KT-*DSL1*	This study
pUA102	pEG-KT-*dsl1-22*	This study
pUA114	YEp13-*YKT6, LEU2, 2*μ*m*	This study
pU6H2MYC	EMBL accession number AJ132965	A. De Antoni
pWB-Acyc*α*	*CYC1-SEC22-myc-α, URA3, CEN6/ARS1*	W. Ballensiefen

sed5-1, and 28% of the *dsl1-22, bos1* (*sec31-1*) double mutants could form colonies. The viability of *dsl1-22* single mutants in these tetrads was higher than 90%. No double mutants were obtained when we tried to combine the *dsl1-22* defect with the *sec20-1*, *sec21-1*, *tip20-5*, *ret1-1*, and *ret1-1*. An unexpected result was the very low viability of all *dsl1-22* spores derived from a diploid heterozygous for *dsl1-22* and sly1^{ts}.

Genomic tagging of the *DSL1* gene was achieved as described by De Antoni and Gallwitz (47) using the oligonucleotides UA1 (5′-AAA CTG AAA AAA AGA CAA CTT ACG CAT ACG TAA TAC AAG ATG TAC ACT ATA GGG AGA CCG GCA GAT C-3′) and UA2 (5′-GCC ATT GAT GAT ATT TAC GAA ATT AGA GGC ACT GCT CTA GAT GAT TCC CAC CAC CAT CAT CAT CAC-3′), whereas the oligonucleotides UA1 and UA3 (5′-ATG TTT TAC AAT GGG GAT TTT TAT CTT TTT GCG ACA GAC GAA CTA ATC TCC CAC CAC CAT CAT CAT CAC-3′) were used for tagging the *dsl1-22* mutant. Plasmids used in this work are listed in Table II.

Synthetic Lethality Screen—Mutants synthetically lethal with *sec22*Δ were isolated using the *ade2/ade8*, red/white sectoring system (48). The SLA28-6C and SUA1-12D strains were red after transformation with pHDS228 on selective plates but gave white sectors under non-selective conditions due to plasmid loss. After mutagenesis with ethyl methane sulfonate 15 non-sectoring colonies could be identified among 200,000 screened. 10 clones were not able to lose the plasmid (*SEC22, URA3*) on 5-FOA plates, and 5 of these did not grow at 37 °C. Three of these allowed the displacement of *SEC22* by *sec22-3*. They were transformed with a *LEU2/CEN*-based yeast genomic library, and one strain showed transformants that sectored and did not contain *SEC22*. The complementing gene was identified by sequencing the ends of the insert and expression of the single ORF.

Sequencing the lsd1-1 (dsl1-22) Mutation—The *lsd1-1* (*dsl1-22*) mutation was cloned by the gap-repair method (49). A 3-kilobase pair fragment (*Xho*I-*Bgl*II) containing *YNL258c* was inserted into the *Xho*I-*Bam*HI sites of pRS315 (*LEU2, CEN6*), and a *Bam*HI-*Sna*BI fragment was removed. The resulting plasmid, which includes DNA that flanks 5′- and 3′-coding regions of *DSL1*, was transformed into the yeast strain YUA1-9C (*MAT*α, *leu2*, *dsl1-22*). Plasmid DNA was isolated from the yeast transformant, amplified in *Escherichia coli*, and subjected to automated sequencing.

Antibodies—The monoclonal anti-c-Myc antibody 9E10 (50) and a polyclonal anti-c-Myc antibody (A-14) were obtained from Santa Cruz Biotechnology. Rabbit antibodies against Sec22p (kindly provided by R. Ossig and R. Grabowski), Emp47p (51), Bet1p, Bos1p, Sed5p, Ypt1p, Sec24p, and BiP/Kar2p were used (52). The polyclonal anti-Ufe1p and anti-coatomer antibodies were gifts from M. Lewis and R. Duden, respectively (Cambridge, UK). Horseradish peroxidase-coupled secondary anti-rabbit or anti-mouse antibodies and cyanine-(Cy2™ or Cy3™)-conjugated secondary antibodies were purchased from The Jackson Laboratories.

Protein Extraction and Immunoblotting—Western blotting analysis was performed as described by Boehm *et al.* (53). Aliquots (1 A_{600} = 1.7×10^7 cells) of transformed cells were lysed in 2 M NaOH, 5% mercaptoethanol and proteins precipitated with 10% trichloroacetic acid, neutralized with 1.5 M Tris base, and dissolved in SDS sample buffer. Proteins were resolved on 12% SDS-PAGE.

Purification of Recombinant Proteins and Affinity Binding Assay—E. coli and *S. cerevisiae* strains expressing GST fusion proteins were lysed, and proteins were solubilized in lysis buffer (20 mM Hepes, pH 6.8, 150 mM KOAc, 5 mM $Mg(OAc)_2$, 1 mM dithiothreitol, 1% Triton X-100, protease inhibitor mix). GST fusion proteins were immobilized on glutathione-Sepharose 4B and washed 5 times with 10 volumes lysis buffer. Proteins bound to GST fusion proteins expressed in yeast were separated by SDS-PAGE and analyzed by immunoblotting. *E. coli* proteins immobilized on glutathione-Sepharose 4B were incubated at 4 °C for 2 h with 100,000 × *g* supernatant of yeast cell lysate. The beads were washed 5 times, and proteins were separated by SDS-PAGE followed by immunoblot analysis.

Subcellular and Sucrose Gradient Fractionation—Yeast cells were harvested at mid-logarithmic phase. The cell pellet was washed twice with water and once with B88 (20 mM Hepes, pH 6.8, 250 mM sorbitol, 150 mM KOAc, 5 mM $Mg(OAc)_2$), resuspended in a minimal volume of B88 containing EDTA-free protease inhibitor mix (Roche Molecular Biochemicals), and pipetted into liquid nitrogen. Cells were ground up in a mortar. The cell powder was resolved in B88 (supplemented with EDTA-free protease inhibitor mix) and centrifuged twice at 500 × *g* for 5 min to remove cell debris, and the clear lysate was centrifuged at 10,000 × *g* for 15 min to obtain the P10 pellet. The S10 fraction was then subjected to centrifugation at 100,000 × *g* at 4 °C for 1 h to obtain P100 and S100. To investigate the membrane localization of Dsl1p, the supernatant of the cell lysate after a 500 × *g* centrifugation was divided into different portions that were treated for 30 min on ice with either 5 M urea, 1% Triton X-100, or 1 M NaCl. The 500 × *g* lysate was also subjected to sucrose density gradient centrifugation.

For fractionation experiments, lysates were loaded on sucrose density gradients (51) and spun at 4 °C in a Beckman SW40 rotor at 37,000 rpm for 2.5 h. 1-ml fractions were taken, and the last fraction was adjusted to 1 ml with B88. Each fraction was mixed with 1 ml of SDS-PAGE sample buffer (8 M urea, 50 mM Tris-HCl, pH 8.0, 2% SDS, 0.1 mg/ml bromphenol blue) and incubated at 50 °C for 10 min prior to analysis by SDS-PAGE and immunoblotting.

Protein Labeling, Immunoprecipitation, and Invertase Assay—For detection of CPY processing cells were shifted to 37 °C for indicated

times, pulse-labeled for 5 min with Tran^{35}S-label (ICN) and chased for 30 min. The labeled proteins were immunoprecipitated using specific antibodies and separated by SDS-PAGE. After incubating the gel with Amplify (Amersham Pharmacia Biotech) for 45 min, the proteins were detected by exposing the gels to X-Omat AR (Eastman Kodak Co.) at −80 °C. Invertase activity staining was carried out as described previously (54).

Fluorescence and Electron Microscopy—Indirect immunofluorescence was performed as described by Schröder *et al.* (51) using rabbit polyclonal anti-Kar2p and monoclonal mouse c-Myc epitope (9E10) antibodies. Cy2™-conjugated goat anti-rabbit or anti-mouse F(ab′) 2 fragment (Jackson ImmunoResearch) served as secondary antibody. DNA was stained with 4′,6-diamidino-2-phenylindole (DAPI). Cells expressing GFP fusion proteins were grown in SD medium at 25 °C to mid-log phase and placed onto a slide. A coverslip was added, and cells were examined immediately. DAPI staining was achieved after fixing cells in methanol at −20 °C for 10 min, washing with acetone at −20 °C, and washing three times with ice-cold PBS, pH 7.4. Confocal images were obtained with a TSC SP1 confocal laser-scanning microscope (Leica). For electron microscopy, yeast cells at mid-logarithmic phase were fixed and stained with permanganate to enhance visualization of membrane structures (54).

RESULTS

Identification of Mutants for Which SEC22 Is Essential—To find proteins that can substitute for Sec22p or to identify factors that prevent these proteins from functioning normally, we performed a synthetic lethality screen. Mutants inviable in the absence of *SEC22* were isolated by using a colony sectoring assay (48). *sec22*Δ mutants that carry a functional *SEC22* gene on the centromeric plasmid pHDS228 were mutagenized. In addition to *SEC22* this plasmid contains the following two markers required for pyrimidine and purine biosynthesis: *URA3* as selectable marker and *ADE8,* which can serve as a color marker in yeast strains carrying mutated versions of the *ADE2* and *ADE8* genes on the chromosomes. The *ade8* mutation is epistatic to *ade2* and prevents the formation of the red color typical for *ade2* mutants. Therefore, cells expressing *ADE8* from a plasmid are red, whereas those that lost the plasmid turn white. As expected, on rich media *sec22*Δ, *ade8, ade2, ura3* cells containing pHDS228 could form white sectors since neither *SEC22*, *ADE8,* nor *URA3* are essential. After mutagenesis, we screened for non-sectoring colonies (for details see "Experimental Procedures"). To confirm that the non-sectoring phenotype in fact reflects a positive selection for the presence of the *SEC22*-carrying plasmid, all mutants were tested for their ability to lose the second plasmid-encoded marker, *URA3*. This test makes use of the drug 5-FOA (5-fluoroorotic acid), which is toxic to Ura$^+$ cells (55). In fact, most of the non-sectoring mutants were sensitive to 5-FOA and only these mutants were analyzed further. In addition to these two phenotypes, five mutants obtained in two independent screens were also temperature-sensitive for growth. Genetic analysis showed that the mutations are recessive and that the inability to lose the *SEC22* gene is tightly linked to the growth defect at 37 °C (see Fig. 1*A*). They belong to three different complementation groups that we called "*LSD1*, *-2,* and *-3*" (lethal with *SEC22* deletion).

We tried to clone the "*LSD*" genes from single copy or multicopy genomic libraries containing *LEU2* as a selectable marker (27). To obtain complementing plasmids, we selected transformants on plates lacking leucine and looked for colonies with white sectors. The formation of white sectors indicated that the cells had again acquired the ability to lose the *SEC22*-carrying plasmid pHDS228. Those transformants, which had simply received an additional copy of *SEC22* from the library, were identified by PCR and discarded. So far our attempts to isolate complementing plasmids from a single copy library were successful only for the "*lsd1-1*" mutant. The library plasmid that we obtained harbored three intact open reading frames.

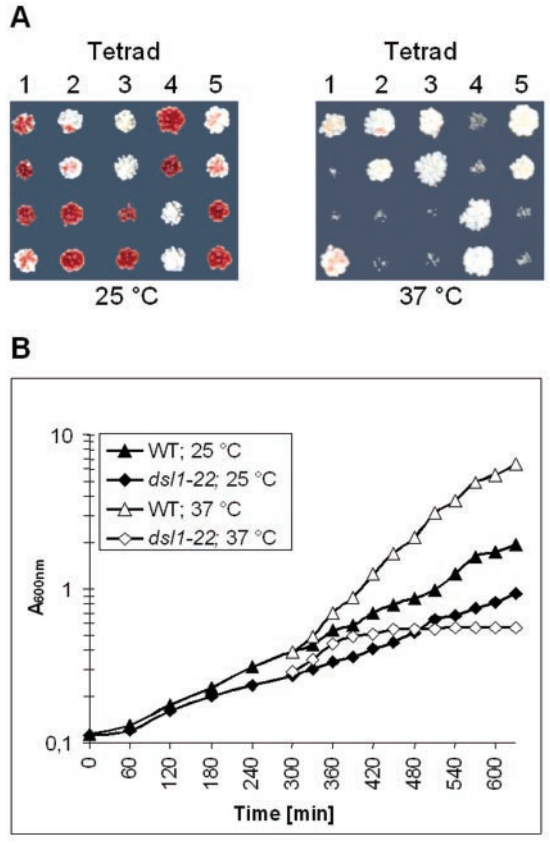

FIG. 1. **Growth characteristics of *dsl1-22* mutant cells.** *A, sec22*::*HIS3*/*sec22*::*HIS3 DSL1*/*dsl1-22, ade2*/*ade2, ade8*/*ade8* heterozygous diploid cells carrying *ADE8* and *SEC22* on a plasmid (pHDS228) were sporulated; spores were separated, and the segregants were incubated on rich medium. Tetrads were replica-plated to low adenine plates and incubated either at 25 or 37 °C. All *red* colonies that are not able to lose the plasmid pHDS228 are temperature-sensitive showing that both defects are closely linked. *B,* growth of wild type (MSUC-3B) and *dsl1-22* (YUA1–9C) cells was monitored by measuring the cell density ($A_{600\ nm}$) during incubation at 25 °C. After 5 h of incubation at 25 °C an aliquot of each sample was shifted to 37 °C for additional 5 h.

Sequencing and subcloning showed that the presence of *YNL258c* alone was sufficient to suppress both the non-sectoring phenotype and the temperature sensitivity of the *lsd1-1* mutant. The open reading frame *YNL258c*, located on chromosome XIV, encodes an essential protein with a predicted molecular mass of 88 kDa with no similarity to other proteins in data bases (56).

The following observations confirmed that defects in *YNL258c* result in a *SEC22*-dependent phenotype as well as a conditional lethal phenotype. Cloning and sequencing of the *lsd1-1* mutant allele revealed the presence of a stop codon at position 2173 of the 2265-base pair long reading frame. This would lead to a gene product, which is 30 residues shorter than the putative wild type protein. By using a PCR-based method described by De Antoni and Gallwitz (47), we replaced *YNL258c* either by a full-length or a shortened version, which were fused to sequences encoding a His_6 epitope followed by two copies of a c-Myc tag. The *Kan*MX cassette inserted downstream of the c-Myc-tagged *YNL258c* sequences served as a selectable marker that allows the transformants to grow in the presence of geneticin (G418). Temperature-sensitive transformants were obtained only when the C-terminally truncated version of *YNL258c* was introduced into wild type cells. Western blotting analysis showed that Ts$^-$ transformants in fact encode a shorter c-Myc-tagged YNL258c protein than cells

expressing the full-length version (data not shown). Tetrad analysis also confirmed that these mutants need *SEC22* for growth (see below). The same results were obtained when N-terminally tagged versions of *YNL258c* and its mutant variant expressed from a centromeric vector were used to complement the deletion of *YNL258c*. In summary, these data established that the deletion of 30 C-terminal triplets from the ORF *YNL258c* results in a conditional lethal phenotype. In cells carrying this mutation the otherwise non-essential *SEC22* gene is rendered essential.

While this work was in progress Waters and co-workers (43) showed that mutations in *YNL258c* can make cells dependent on the *SLY1-20* mutation. The mutants identified were accordingly named *dsl1-1* to *dsl1-7* (*d*ependent on *SLY1-20*). *SLY1-20* is a dominant mutation, which suppresses the defects in several yeast mutants affected in ER-to-Golgi transport (27, 37, 57–60). Accordingly, the mutant we obtained was renamed *dsl1-22.* Consistent with the results obtained by VanRheenen *et al.* (43), the temperature sensitivity of *dsl1-22* is suppressed by the *SLY1-20* mutation on a single copy plasmid (data not shown).

Genetic Interaction of dsl1-22 with Other Genes Whose Products Act in ER-Golgi Anterograde and Retrograde Transport—In the process of cloning out sequences able to complement the *dsl1-22* mutation, we also obtained clones from multicopy libraries. Among these clones were plasmids containing the *YKT6* gene. *YKT6* encodes a lipid-anchored member of the synaptobrevin family of SNARE proteins (61). This prompted us to test whether the overexpression of other SNARE-encoding genes has similar effects.

We found that, similar to the results obtained with *YKT6,* overexpression of *SED5* allowed *dsl1-22* mutants to tolerate the loss of *SEC22*. However, the overexpression of neither *YKT6* nor *SED5* was able to suppress the Ts$^-$ phenotype of *ds11-22* mutants. Overexpression of the other SNARE-encoding genes specific for ER-Golgi transport, *BET1*, *BOS1* or *UFE1,* was unable to suppress the non-sectoring phenotype of *dsl1-22* mutants.

The approach, which led to the isolation of the *dsl1-22,* was based on the synthetic lethality of the *dsl1-22* mutation when combined with the *sec22* deletion. Therefore, we also addressed the question whether *dsl1-22* is synthetically lethal with other defects in ER-to-Golgi transport. For this and all subsequent assays we used *dsl1-22* mutants expressing *SEC22* from its normal locus on chromosome XII: (i) a strain obtained by backcrossing cells derived from the original mutant (Fig. 1*A*) twice to wild type cells (*SEC22*), and (ii) a mutant in which we had introduced *dsl1-22-myc* construct at the *YNL258c* locus (see above). The analysis of tetrads was greatly facilitated by the presence of the *Kan*MX cassette closely linked to the *dsl1-22-myc* allele which thus allowed us to identify the *dsl1-22* mutants by their resistance to G418.

Viable double mutants were obtained when we combined the *dsl1-22* defect with *sec23-1*, *sec22-3*, *bet1-1*, *sed5-1, bos1* (*sec31-1*), and *sec27-1* mutations. The first mutation leads to a block in anterograde ER-to-Golgi transport due to a defect in COPII assembly (62); *bet1-1*, *sec22-3,* and *sed5-1* are mutations that affect genes encoding SNARE proteins involved in ER-Golgi transport, whereas *SEC27* encodes a COPI component (63). The number of viable double mutants obtained differed to a great extent as determined by complementation assays and analyzing their resistance to G418 (for details see "Experimental Procedures"). The observation that *sec22-3*, *dsl1-22* double mutants are viable whereas *dsl1-22* mutants are inviable in the absence of *SEC22* was confirmed by plasmid shuffling experiments using a *dsl1-22* mutant and *SEC22* or *sec22-3* containing plasmids (data not shown). This finding illustrates that this assay is specific for certain alleles. Therefore, missing or weak genetic interactions mentioned above do not rule out that the gene products perform a related function. This may be true at least for *BOS1* and *DSL1* since all the *bos1* (*sec31-1*), *dsl1-22* double mutants that we obtained formed very small colonies. No double mutants were obtained when diploids heterozygous for the *dsl1-22* and the *sec22*Δ, *sec21-1*, *ret1-1*, *ret1-1*, *sly1^{ts}*, *sec20-1,* or *tip20-5* mutations were subjected to tetrad analysis. The *sec21-1* (γ-COP), *ret1-1* (α-COP), *ret1-1* (δ-COP), *sec20-1,* and *tip20-5* mutants primarily affect the retrograde transport from Golgi to ER, and defects in forward transport may be secondary (20, 22, 24, 32, 33). The strong genetic interaction between *dsl1-22* and these mutations indicates that *DSL1* may be required for Golgi-ER retrograde transport. The synthetic lethality of *dsl1-22* and *sly1^{ts}* are consistent with the observation made by VanRheenen *et al.* (43) who isolated *dsl1* mutants that depend on a dominant *SLY1* mutation.

The dsl1-22 Mutant Shows Slight Defects in Forward Transport—The *dsl1-22* mutant cells gave rise to slightly smaller colonies than wild type cells even at room temperature. Accordingly, the growth rate of *dsl1-22* mutant cells is slower when measured in liquid culture (Fig. 1*B*). Growth of *dsl1-22* mutants stops completely 2 h after a shift to 37 °C. This Ts$^-$ phenotype allowed us to examine the function of Dsl1p in the secretory pathway at restrictive temperatures. First we analyzed the secretion of periplasmic invertase in wild type and *dsl1-22* cells at different times after shifting cells to 37 °C. Measuring total invertase activity using intact and permeabilized cells (64) showed that the ratio of secreted to intracellular invertase does not change significantly up to 3 h after the shift to 37 °C (data not shown). To detect a possible glycosylation defect due to slower ER-to-Golgi transport in *dsl1-22* mutants, intracellular and extracellular fractions of wild type and mutant cells were separated by non-denaturing PAGE. Invertase was visualized by an activity stain. As shown in Fig. 2*A, dsl1-22* cells secrete partially underglycosylated invertase even at 25 °C. The shift to the restrictive temperature leads to some accumulation of the ER core-glycosylated form inside the cell. For comparison, at restrictive temperature the *sec22-3* mutation also leads to the intracellular accumulation of core-glycosylated invertase and secretion of a small amount of underglycosylated enzyme. An incomplete block in anterograde transport also became evident when the maturation of the vacuolar protease CPY was analyzed in *dsl1-22* cells (Fig. 2*B*). In pulse-chase experiments CPY appears first as a p1 precursor in the ER, is then modified to a larger form, p2, in the Golgi, and is transported to the vacuole where it is processed to its mature form (m) by proteolysis. As expected, *sec22-3* mutant cells show a complete block in ER-to-Golgi transport 15 min after the shift to 37 °C. In this mutant only the ER form (p1) is visible consistent with a complete block in ER-to-Golgi transport. In *dsl1-22* cells about half of CPY is still normally processed even 3.5 h after the shift to 37 °C. This corresponds to the results observed with other temperature-sensitive alleles of *DSL1* (43).

dsl1-22 Cells Accumulate ER Membranes but Not Vesicles at Restrictive Temperature—The morphology of wild type and *dsl1-22* cells incubated at 25 or 37 °C was compared by electron microscopy. As shown by Kaiser and Schekman (36), mutants with defects in the budding reaction accumulate membranes, whereas mutants that exhibit defects in fusion of vesicles with target membranes accumulate vesicles. At 25 °C the morphology of *dsl1-22* cells does not differ significantly from that of wild type cells grown at 37 °C (Fig. 3, *A* and *B*). Fig. 3*C* shows a representative micrograph of a *dsl1-22* mutant cell after

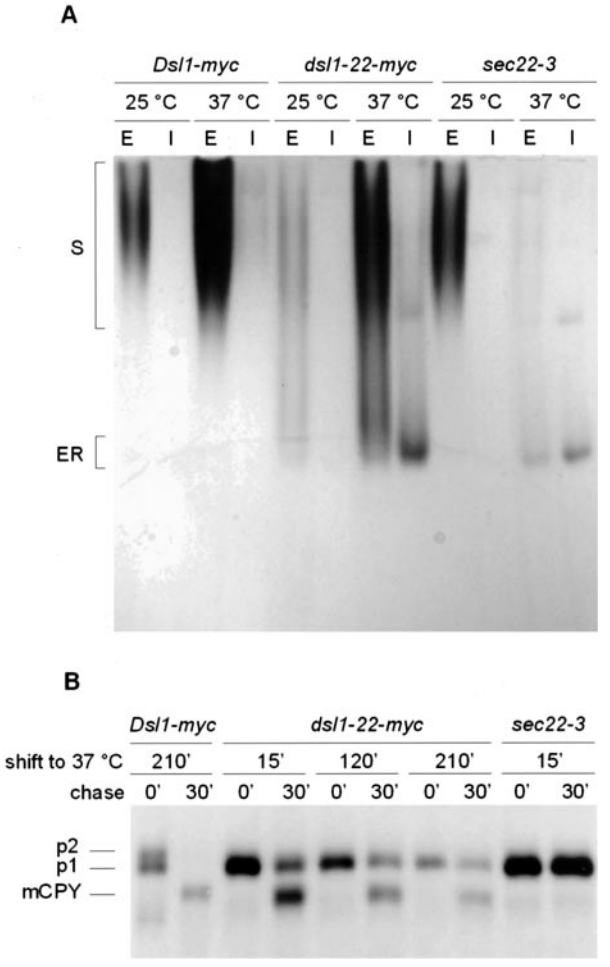

FIG. 2. **dsl1-22 cells exhibit mild defects in anterograde ER-to-Golgi transport.** *A,* fate of secreted invertase in *dsl1-22* cells. Invertase synthesis was induced for 30 min in wild type (*Dsl1-myc*; YUA11), *dsl1-22-myc* (YUA41), and *sec22-3* cells (SHC21-12A) either at 25 or 37 °C. Preincubation at 37 °C started 30 min before induction. Glycosylation level of the enzyme in intracellular (*I*) and extracellular fractions (*E*) was detected by an activity stain in non-denaturing gels. The position of highly glycosylated invertase (*S*) and ER core-glycosylated invertase (*ER*) is indicated. *B,* intracellular processing of carboxypeptidase Y in wild type (YUA11) and mutant cells (YUA41 and SHC21-12A). Cells were shifted to 37 °C for indicated times, pulse-labeled with [^{35}S]methionine/cysteine for 5 min, and chased for 0 and 30 min. The cells were lysed; CPY was immunoprecipitated, and proteins were resolved by SDS-PAGE.

incubation at the nonpermissive temperature for 90 min. Compared with wild type cells (Fig. 3*A*) *dsl1-22* cells show a strong accumulation of membranes, which mainly emerge from the ER contiguous with the nuclear membrane (Fig. 3, *C* and *D, arrow*). Similar structures also originate from cortical endoplasmic reticulum close to the plasma membrane (Fig. 3*D*, *arrowhead*). No significant increase in the number of small vesicles was observed. Thus, *dsl1-22* mutants very much resemble the coatomer mutant *sec27-1* (63).

dsl1-22 Mutants Are Defective in the Retrieval of ER Proteins from the Golgi—The strong genetic interaction of the *dsl1-22* defect with mutations affecting retrograde Golgi-to-ER transport and the incomplete block in anterograde transport when growth already had ceased indicated that the primary function of Dsl1p could be in the retrieval of proteins from the Golgi complex. Therefore, we employed different assays to compare retrograde transport in wild type and *dsl1-22* cells.

Mutants affecting genes required in retrograde transport like *SEC20* and *SEC22* secrete large amounts of the soluble ER protein BiP/Kar2p (65). Fig. 4*A* shows that the same is true for

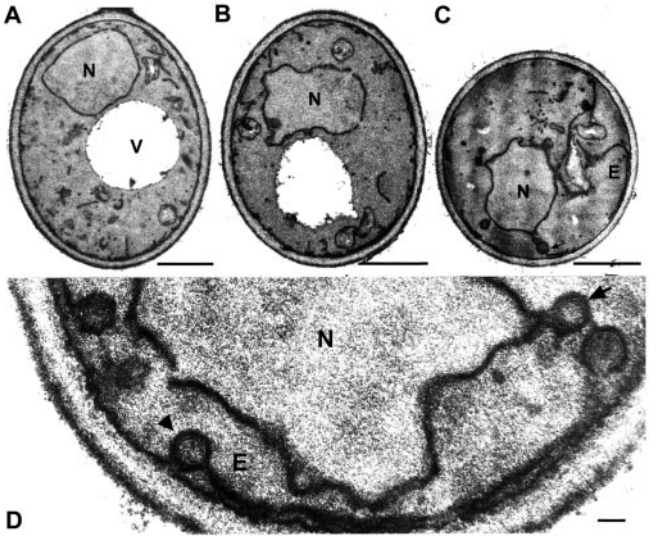

FIG. 3. **Electron micrographs of wild type and *dsl1-22* cells.** Wild type cells (MSUC-3B) grown at 37 °C for 90 min were used as a control (*A*). Mutant cells (YUA1-9C) grown at 25(*B*) or 37 °C for 90 min (*C* and *D*) were fixed with potassium permanganate to highlight membrane structures. Typical cells are shown for each condition. The *arrowhead* in *D* points to membranes emanating from the cortical ER (*E*), whereas arrows in *C* and *D* indicate sites of membrane accumulation at the nucleus (*N*). *V*, vacuole. *Bars,* 1 μm in *A–C*; 0.1 μm in *D*.

dsl1-22 and *dsl1-22-myc* mutants. This defect in BiP/Kar2p localization was also observed by immunofluorescence microscopy using an affinity-purified polyclonal anti-BiP/Kar2p antibody. In wild type cells BiP/Kar2p antibodies stain the nuclear periphery which is the characteristic ER staining in yeast (66). In contrast to the typical ER staining in wild type cells, we could observe a dot-like pattern in *dsl1-22* cells even at permissive temperature (Fig. 4*B*), similar to "BiP bodies" observed in several ER-to-Golgi mutants at restrictive temperature (67).

To examine the defect in retrograde transport more specifically, we focused on the targeting of the SNARE protein Sec22p. As described previously (18, 46) α-factor fused to Sec22p through a Kex2p cleavage site, and a c-Myc epitope is a suitable tool for analyzing targeting of Sec22p. Several recycling mutants exhibit mislocalization of Sec22-α (18) resulting in cleavage by the late Golgi protease Kex2p. The removal of the α-factor reporter from Sec22p is easily detected by immunoblot analysis. Fig. 4*C* shows the steady state processing of Sec22-α in wild type, *dsl1-22* and *dsl1-22-myc* strains incubated at 25 °C. About 75% of Sec22-α proteins was cleaved by Kex2p in mutant cells, whereas very little of the reporter was cleaved by Kex2p in wild type cells. Pre-shifting cells to 37 °C for 2 h did not result in a more efficient cleavage (data not shown). It is unlikely that more efficient cleavage of Sec22-α in *dsl1-22* is due to some Kex2p activity in the ER since mislocalization of a Sec22p-derived fusion protein was also obvious when we analyzed cells producing a GFP-tagged Sec22 protein (Fig. 4*D*). This fusion protein is fully functional since it is able to suppress the growth defect of *sec22-3* mutants (data not shown). Moreover, GFP-Sec22p behaves like C-terminally tagged Sec22 proteins when analyzed in wild type and *ufe1-1* mutant cells (Fig. 4*D*; see Ref. 18). In wild type cells fluorescence appeared as a ring around the nucleus which represents ER, whereas in *dsl1-22* cells a punctated staining was detectable, very likely representing Golgi structures (18). As with other recycling mutants, this defect already occurs at 25 °C (20). Taken together, both the efficient Kex2p processing of Sec22-α and the localization of GFP-Sec22 indicate that *dsl1-22* mutants are defective in ER retention of Sec22p.

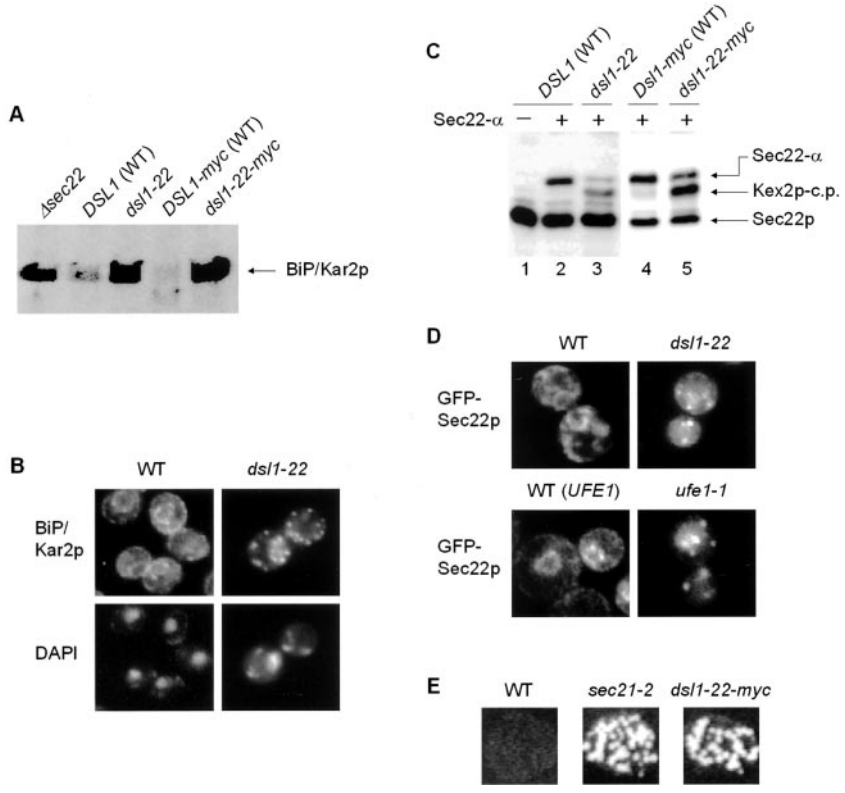

FIG. 4. **Mislocalization of different ER proteins in *DSL1* mutant cells.** *A,* wild type (*DSL1*, MSUC-7C, and *DSL1-myc*, YUA11) or *dsl1-22* mutant cells (*dsl1-22*, YUA1-9C, and *dsl1-22-myc,* YUA41) were transferred into fresh YPD medium and grown at 25 °C. At $A_{600\ nm}$ of 1.0 cells were removed from the medium by centrifugation, and proteins in the medium were precipitated by the addition of 10% trichloroacetic acid (final concentration). Proteins were resolved by SDS-PAGE and analyzed by Western blotting using polyclonal anti-BiP/Kar2p antibodies. *B,* wild type (MSUC-3B) and *dsl1-22* (YUA1-9C) cells were grown to an early log phase at 25 °C, fixed, and stained with affinity purified anti-BiP/Kar2p antibody (*upper panels*). In addition, DAPI staining was used to localize the nuclei (*lower panels*). *C,* Sec22-α processing by the late Golgi protease Kex2p. Immunoblot analysis was performed with extract from wild type (*DSL1*, MSUC-7C, and *DSL1-myc*, YUA11) or *dsl1-22* mutant cells (*dsl1-22*, YUA1-9C, and *dsl1-22-myc,* YUA41) transformed with pWB-Acycα as indicated. Aliquots of cells were harvested after overnight incubation at 25 °C in selective medium, and proteins were analyzed by Western blotting. A polyclonal anti-Sec22p serum was used to detect the Sec22p-derived hybrid protein (Sec22-α), its Kex2p cleavage product (*Kex2p-c.p.*), and the endogenous Sec22 protein. *D,* confocal images of unfixed cells expressing GFP-Sec22p grown at 25 °C. Images show the cellular distribution of GFP-Sec22p in wild type (*Dsl1-myc*, YUA11), *dsl1-22-myc* cells (YUA41), *UFE1* wild type cells (MLY-100), and *ufe1-1* mutant cells (MLY101). *E, dsl1-22* cells are defective in ER retrieval of Ste2-Wbp1p. *MAT***a** *ste2*Δ yeast cells expressing Ste2-Wbp1p were grown on YPD plates and replica-plated to a lawn of *MAT*α cells. After 6 h at 30 °C to allow mating, cells were replica-plated to SD plates selective for the growth of diploid cells only. *sec21-2* (PC82) and *dsl1-22-myc* (SUA5) mutants were able to form diploids, whereas wild type (*WT*) (STE2-4B) cells could not mate with the tester strain (MSUC-2D).

To examine whether the *dsl1-22* mutation also interferes with the ER retention of type I transmembrane proteins carrying the KK*XX* retrieval signal, we performed the Ste2-Wbp1-dependent mating assay described by Letourneur *et al.* (20). We introduced the *dsl1-22-myc* allele into a strain expressing a KK*XX*-tagged version of the α-factor receptor (Ste2-Wbp1p) instead of the wild type *STE2* gene. Wild type cells of mating type **a** expressing only this receptor cannot mate with cells of mating type α since Ste2-Wbp1p is efficiently retained in the ER due to the KK*XX*-tag fused to the C terminus. Mutants that mislocalize the receptor to the plasma membrane can form diploids with a suitable tester strain. With the Ste2-Wbp1-based assay efficient mating occurs for instance in *sec21-2* (γ-COP) mutants (see Ref. 20; see also Fig. 4*E*). Fig. 4*E* shows that *dsl1-22-myc* cells producing Ste2-Wbp1p can mate as efficiently as the *sec21-2* mutants indicating that targeting of KK*XX*-tagged ER proteins is impaired already at a permissive temperature of 30 °C. In summary, the data show that *dsl1-22* mutants are defective in the ER retention of different types of proteins: soluble HDEL carrying proteins like BiP/Kar2p, type II transmembrane proteins like the *v*-SNARE Sec22p, as well as type I transmembrane proteins carrying a KK*XX* retrieval signal.

Subcellular Distribution of Dsl1p—According to its primary sequence, Dsl1p contains no putative transmembrane domains. Extracts from Dsl1-*myc* producing cells (YUA11) were used to examine a possible membrane association of Dsl1p. A 500 × *g* supernatant of cell lysate was treated either with buffer (B88), 5 M urea, 1% Triton X-100, or 1 M NaCl and subsequently centrifuged at 10,000 × *g* and 100,000 × *g* (Fig. 5). When incubated with buffer alone, no Dsl1-*myc* was detectable in the soluble fraction, whereas both urea and detergent treatment led to solubilization of Dsl1-*myc*. Less than 5% of the total amount of Dsl1-*myc* became soluble upon treatment with high salt suggesting that Dsl1p is a peripherally associated membrane protein. In contrast, the transmembrane protein Sec22p could only be solubilized by detergent. Experiments using a recently obtained Dsl1-specific serum gave identical results (data not shown).

Next we performed subcellular fractionation studies using sucrose density gradients to compare the localization of Dsl1p with that of known Golgi- and ER-resident proteins. Cell lysates of strain YUA11 (*DSL1-myc*) were prepared and loaded on top of sucrose gradients, and fractions were collected after centrifugation as described under "Experimental Procedures." Fig. 6, *A* and *B,* shows that Emp47p, a Golgi marker, the ER resident t-SNARE Ufe1p, as well as the ER-marker BiP/Kar2p display characteristic distributions (51, 24, 66). Like Ufe1p and BiP/Kar2p Dsl1-*myc* protein was detectable exclusively in the dense fractions when using the monoclonal anti-c-Myc anti-

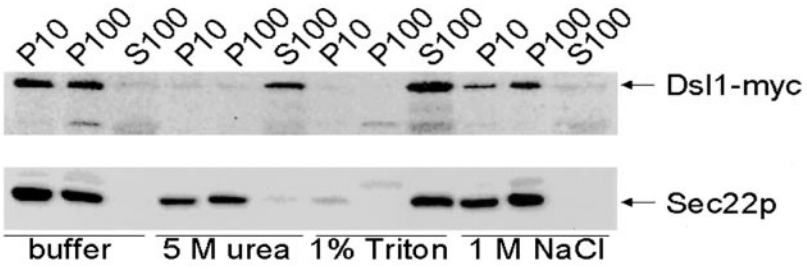

FIG. 5. **Dsl1p is a peripheral membrane protein.** Logarithmically grown cells of YUA11 (*DSL1-myc*) were disrupted using glass beads. The lysate (500 × *g* supernatant) was treated as indicated (see "Experimental Procedures") and then centrifuged at 10,000 and 100,000 × *g*. The resulting pellet (*P10* and *P100*) and supernatant (*S100*) fractions were resolved on a 12% polyacrylamide gel and immunoblotted with anti-Sec22p and anti-c-Myc antibody (9E10). In contrast to the integral membrane protein Sec22p, Dsl1-*myc* became soluble after incubation with 5 M urea.

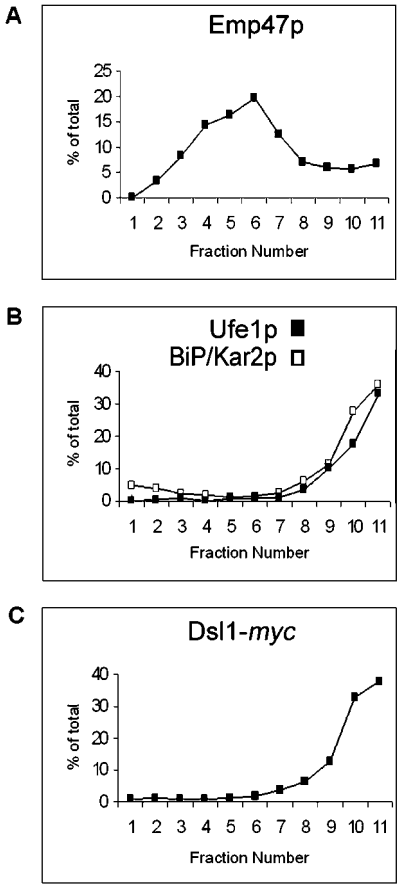

FIG. 6. **Dsl1p cofractionates with ER markers in sucrose velocity gradients.** Lysates of strains YUA11 (*DSL1-myc*) grown at 25 °C were loaded on 18–60% sucrose density gradients. After centrifugation, fractions were collected and subjected to Western blot analysis with antibodies directed against Emp47p, a Golgi marker (*A,* see Ref. 51), Ufe1p and BiP/Kar2p, two ER markers (*B,* see Refs. 24 and 66), and c-Myc to detect tagged Dsl1 protein expressed at wild type levels (*C*). The data represent average values from at least two experiments.

body 9E10 directed against the c-Myc epitope, presumably reflecting ER localization (Fig. 6*C*).

Dsl1p Interacts Physically with Coatomer—To get additional clues for the involvement of Dsl1p in retrograde and/or anterograde ER-to-Golgi transport, we investigated possible interactions of Dsl1p with proteins involved in these trafficking steps. First we tried to address this question by expressing Dsl1p tagged with glutathione *S*-transferase (GST) in yeast. The 100,000 × *g* supernatants from detergent-lysed yeast cells (YUA11) expressing GST or GST-Dsl1p were loaded on glutathione-Sepharose 4B to immobilize GST or GST-Dsl1p and associated proteins. After washing the beads to remove unbound proteins, antibodies were used to monitor the binding of several ER/Golgi proteins to Dsl1p. Anti-coatomer antibodies resulted in very strong signals (data not shown), whereas only weak signals were obtained with Emp47p-specific antibodies. These signals were specific for the Dsl1 part of the fusion protein since no binding was observed when lysates from GST-expressing cells were analyzed. The SNARE proteins Bet1p, Bos1p, Sec22p, and Sed5p as well as the COPII component Sec24p and the Rab-like GTPase Ypt1p were not retained on the affinity matrix in significant amounts.

To verify and extend these findings, we incubated extracts of detergent-lysed yeast cells with different GST fusion proteins purified from *E. coli.* In line with the results obtained with GST fusion proteins expressed in yeast, coatomer (COPI) showed strong binding to GST-Dsl1p. Notably, coatomer recruitment to GST-Dsl1p from *E. coli* takes place even at 4 °C (see "Experimental Procedures"), a temperature where enzymatic activities are low. As controls, GST, GST-Sed5p, GST-Bos1p, or GST-Sec22p were not able to recruit coatomer from cell lysates (Fig. 7). Very faint bands representing coatomer were seen when GST-Tip20p was loaded on glutathione-Sepharose 4B (Fig. 7*B*, *lane 5*). Dsl1p may mediate this indirect binding between GST-Tip20 and coatomer because Ito *et al.* (68) recently showed that Tip20p and Dsl1p interact in two-hybrid assays. However, so far we could not observe direct binding of Dsl1-*myc* to GST-Tip20p *in vitro*. In addition, Dsl1-*myc* did not bind to GST-Bos1p, GST-Sec22p, or GST-Sed5p (data not shown). Likewise, GST-Dsl1p was not able to bind Bet1p, Bos1p, Sec22p, Sed5p, Ypt1p, Sec24p, or Emp47p, suggesting that the weak binding of Emp47p mentioned above could be indirect via coatomer.

DISCUSSION

Genetic Analysis Indicates That Dsl1p Is Required for Retrograde Golgi ER Traffic—In the present study we identified a novel mutation that renders cells dependent on the otherwise dispensable SNARE protein Sec22p. This mutation makes cells temperature-sensitive for growth, allowing us to analyze the function of the affected gene. Cloning and sequencing showed that this mutant is a new allele of the essential open reading frame *YNL258c*, encoding a truncated protein that lacks its 30 C-terminal residues.

Recently, mutant alleles of *YNL258c,* named *dsl1-1* and *dsl1-2,* were identified by VanRheenen *et al.* (43) as mutations that make yeast cells dependent on the dominant suppressor mutation of *SLY1*, *SLY1-20*. Thus, screening for genetic defects that confer dependence on either Sec22p or on the dominant *SLY1-20* mutation led to the identification of the same gene, *DSL1*. By comparing the results, the Sec22p-dependent *dsl1-22* mutant has similar properties as the PCR-generated temperature-sensitive alleles *dsl1-5* and *dsl1-6* obtained by VanRheenen *et al.* (43). They show a slight defect in ER-to-Golgi transport of CPY, and their growth defect at 37 °C can be suppressed by the *SLY1-20* mutation. However, the mutants obtained using the two approaches differ in several other phe-

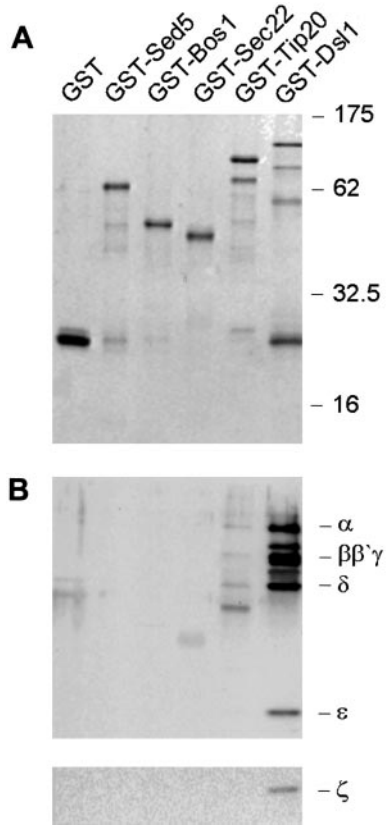

FIG. 7. **Specific binding of coatomer subunits to GST-Dsl1p.** Proteins from detergent-lysed yeast cells were incubated at 4 °C for 2 h with GST alone or GST fusion proteins purified from *E. coli* and immobilized on glutathione-Sepharose 4B. Beads were washed 5 times (see "Experimental Procedures"), and the proteins bound were analyzed by SDS-PAGE followed by Coomassie Blue staining (*A*) and immunoblot analysis using a polyclonal antibody against coatomer (*B*). The positions of molecular weight markers and the different COPI subunits are indicated.

notypes. The *SEC22*-dependent *dsl1-22* mutant is temperature-sensitive, and defects in vesicular transport could thus be analyzed directly. The *SLY1-20*-dependent mutants *dsl1-1* and *dsl1-2* are not Ts^- and display secretory defects only after expression of the *SLY1-20* allele is shut off. Another difference concerns the suppression of the non-sectoring phenotype. The dependence of the *dsl1-1* mutant on *SLY1-20* could not be suppressed by overexpression of the t-SNARE-encoding *SED5* gene (43), whereas *SED5* overexpression in *dsl1-22* cells could eliminate the requirement for Sec22p. This observation may imply a direct functional link between Dsl1p and SNARE proteins like Sec22p and Sed5p.

Both Sec22p and Sed5p show strong genetic interactions with genes encoding proteins involved in Golgi-ER retrograde transport (37, 69, 70). Double mutant analysis revealed that the same is true for *dsl1-22*. During our attempts to create double mutants harboring the *dsl1-22* mutation combined with additional mutations affecting the ER-Golgi transport cycle, we observed the strongest genetic interactions of *dsl1-22* with mutations affecting retrograde Golgi-to-ER transport. No double mutants were obtained when we crossed *dsl1-22* strains with mutants affected in coatomer subunit-encoding genes like *RET1* (α-COP), *RET2* (δ-COP), and *SEC21* (γ-COP) or with mutants in *SEC20* and *TIP20* which are important for fusion of Golgi-derived vesicles with the ER (32, 33). In accordance with this, VanRheenen *et al.* (43) found that overexpression of the γ-COP-encoding *SEC21* gene partially suppresses the Ts^- defect of *dsl1* mutants. Together these results strongly suggest that Dsl1p may play a role in Golgi-ER retrograde traffic. One could speculate that the need for Sec22p displayed by the *dsl1-22* mutant may be due to the mislocalization of SNARE proteins that can functionally replace Sec22p. This is also indicated by the fact that the requirement for Sec22p at least at room temperature can be alleviated either by excess of Ykt6p or Sed5p, two other SNARE proteins. As discussed below, Sec22p as well as Bos1p are in fact mislocalized in *dsl1-22* cells. Unexpectedly, *SEC22* can be replaced in *dsl1-22* mutants by the *sec22-3* allele. This was surprising since the *sec22-3* point mutation has stronger effects on the growth of certain strains than the deletion of *SEC22* (*sec22*Δ cells that are not Ts^- can become temperature-sensitive after introducing a *sec22-3*-containing plasmid).[2]

dsl1-22 Mutants Have a Strong ER Retention Defect—In *dsl1-22* cells maturation of the vacuolar hydrolase CPY is only partially inhibited, similar to what has been described for the PCR-generated *dsl1-5* and *dsl1-6* mutants (43). Invertase secretion is almost normal in *dsl1-22* mutants and a slight inhibition of anterograde transport is indicated by the accumulation of a small amount of core-glycosylated invertase. Electron microscopy analysis of mutant cells reveals a severe accumulation of membranes emerging from the ER after shift to nonpermissive temperature. Similar structures were observed in a β′-COP mutant, *sec27-1* (63). Since the morphology of *dsl1-22* mutant cells is almost normal at 25 °C, a temperature at which retrograde transport is already affected (see below), this EM phenotype at restrictive temperature is likely to be a more indirect effect due to perturbed forward transport.

The weak inhibitory effect on forward transport appears to be a result of a strong defect in retrograde transport back to the ER. In *dsl1-22* cells this block is already seen at permissive temperature, consistent with what has been seen with other recycling mutants (18, 20, 22). The *dsl1-22* mutant allele affects the retrieval of recycling SNARE proteins, proteins sorted by their C-terminal KK*XX* motif, and the soluble ER protein BiP/Kar2p, whose recycling depends on the HDEL receptor Erd2p (65). How can retrograde transport defects have an effect on forward transport? Obviously, one possibility is that components of the vesicle budding and fusion machineries may become limiting due to their mislocalization. In addition, it is known that exit from the ER requires the proper folding of cargo molecules, and this in turn depends on chaperones like BiP/Kar2p or PDI (71, 72). These chaperones carry a C-terminal HDEL signal that mediates their retention in the ER. In *dsl1-22* mutant cells, BiP/Kar2p and very likely PDI are not properly retained in the ER. Insufficient amounts of BiP/Kar2p and PDI in the ER could retard the exit of cargo molecules (71, 72).

The following results demonstrated that *dsl1-22* cells are defective in Golgi-to-ER-retrieval of Sec22p. A GFP-tagged version of Sec22p localizes to the ER in wild type cells, whereas in *dsl1-22* cells GFP-Sec22p displays a punctate staining pattern typical for Golgi markers. The Sec22-α fusion protein reaches the late Golgi apparatus in *dsl1-22* cells but not in wild type cells as indicated by its Kex2p-dependent cleavage. Fractionation studies with sucrose density gradients showed that Bos1p exhibits a shift from ER-to-Golgi fractions in *dsl1-22* cells compared with wild type cells (data not shown). Mislocalization of the soluble ER marker BiP/Kar2p was also demonstrated using immunofluorescence and a secretion assay. BiP/Kar2p fluorescence in *dsl1-22* mutant cells shows a punctate pattern. Similar, more randomly distributed structures were described previously for several *sec* mutants and were named BiP bodies

[2] T. Neumann, unpublished results.

(67). These authors suggested that BiP bodies could be exit sites where leaving proteins accumulate in different mutant strains due to low efficiency of Golgi-to-ER retrieval. Some mutants even secrete Kar2p into the medium. Indeed, this phenomenon can be observed with *dsl1-22* mutant cells. The level of Kar2p secretion by these cells is comparable to that of *sec22-3*, *sec22*Δ, *sec20-1* cells (65).[3]

Besides mislocalization of SNARE proteins and of the luminal ER protein BiP/Kar2p, *dsl1-22* cells exhibit also defects in retrieval of proteins sorted by their C-terminal KK*XX* motif. In this study we used Ste2-Wbp1p as a marker protein (20). Our results implicate Dsl1p in retrograde transport of dilysine-tagged proteins from the Golgi compartment to the ER. We also analyzed the localization of Emp47p, a Golgi protein carrying a variant of the dilysine-motif, KXK*XX* (51). Unlike Ste2-Wbp1p, the localization of Emp47p is unaffected in *dsl1-22* cells. This is indicated by the results of gradient fractionation and immunofluorescence experiments (data not shown). In this respect, *dsl1-22* mutants resemble *ret1* (α-COP) mutants that also mislocalize KK*XX*-tagged proteins of the ER but not the KXK*XX*-tagged Emp47p (23).

The Localization of Dsl1p Is Still Unclear—Dsl1p is a peripheral membrane protein that can be solubilized with 5 M urea and colocalizes with ER marker proteins in sucrose density gradients. Fractionation experiments were performed with a c-Myc-tagged Dsl1 protein expressed at wild type levels. These results were later confirmed using antibodies raised against bacterially produced Dsl1 protein. We also tried to determine the localization of Dsl1p by immunofluorescence. Unfortunately, affinity purified polyclonal antibodies against Dsl1p still exhibited strong cross-reactivities and were thus not helpful for immunofluorescence analysis. Specific signals were only obtained when tagged versions of Dsl1p were overproduced. The expression of GFP-Dsl1p led to fluorescence pattern varying from Golgi-like staining consisting of a few large dots in cells from early logarithmic growth phase to nuclear staining at $A_{600\,nm} > 1$. Overexpression of c-Myc-tagged Dsl1p led to diffuse punctate fluorescence. A cytoplasmic staining consisting of many small dots was also observed for Tip20p, which is cytoplasmic when overproduced. Tip20p could be recruited to the ER when Sec20p was overproduced as well (73). Given the tight genetic (see above) and direct interactions (68) between Tip20p and Dsl1p they may behave similarly. Unlike Tip20p, overproduced Dsl1p does not localize to the ER when *SEC20* was overexpressed simultaneously (data not shown).

Dsl1p Interacts Strongly with Coatomer—As mentioned above, a recent systematic yeast two-hybrid study revealed direct interactions of Dsl1p with Tip20p (68). Dsl1p showed interactions with several other proteins. However, only in the case of Dsl1p and Tip20p, this interaction was observed with Dsl1p as bait as well as prey, *i.e.* both fusion orientations. This is consistent with the genetic data since the *tip20-5* defect is synthetically lethal in combination with *dsl1-22* (this study). The genetic as well as physical interaction between *DSL1* and *TIP20* and their gene products suggest that both proteins could be involved in the same transport step. Tip20p is able to bind to the cytosolic region of Sec20p (73). Together they form a complex with the SNARE proteins Ufe1p and Sec22p (32). This unconventional SNARE complex is involved in retrieval of dilysine-tagged proteins from Golgi to ER (33). In summary, Dsl1p interacts directly with Tip20p (68), and the *dsl1-22* mutation exhibits synthetic lethality in combination with *sec22*Δ, *sec20-1,* and *tip20-5*. Synthethic-lethal genetic interaction between mutations in *SEC22*, *SEC20*, *TIP20,* as well as *UFE1* and mutations affecting coatomer subunits were established previously (69).

As expected, *dsl1* mutants also exhibit genetic interactions with coatomer mutants (see Ref. 43; this study). Final evidence for Dsl1p playing an important role in retrograde Golgi-ER traffic is our finding that Dsl1p interacts physically with coatomer. Coatomer could be copurified with GST-Dsl1p from yeast cells, and it could be recruited from yeast lysates to recombinant GST-Dsl1p purified from *E. coli.* No additional factors present in the cell extracts were required for this interaction since purified coatomer can also bind to GST-Dsl1p (data not shown). Interestingly, the C-terminal truncated mutant protein, Dsl1-22p, which leads to a defect in retrograde transport, is still able to bind all coatomer subunits with an affinity comparable to the full-length protein (data not shown). Thus the C terminus of Dsl1p is not essential for binding of coatomer but perhaps could represent a binding region for other proteins involved in these transport steps.

Considering the fact that Dsl1p binds coatomer as well as Tip20p, a component of the putative docking complex at the ER, we suggest that Dsl1p is involved in a step between uncoating and docking. It will be important to determine whether Dsl1p can bind both coatomer and Tip20p at the same time or whether the interaction is sequential.

Acknowledgments—We thank François Letourneur, Renwang Peng, and Anna De Antoni for providing plasmids and yeast strains. We thank Anne Spang and Rainer Duden for critical comments on the manuscript. We thank Stefan Jakobs for help with the confocal microscope, H.-H. Trepte for electron microscopy, Mike Lewis and Rainer Duden for antibodies, Hans-Peter Geithe for sequencing, Hannegret Frahm for technical assistance, and Dieter Gallwitz for support.

REFERENCES

1. Rothman, J. E., and Warren, G. (1994) *Curr. Biol.* **4,** 220–233
2. Schekman, R., and Orci, L. (1996) *Science* **271,** 1526–1533
3. Cao, X. C., Ballew, N., and Barlowe, C. (1998) *EMBO J.* **17,** 2156–2165
4. Guo, W., Sacher, M., Barrowman, J., Ferro-Novick, S., and Novick, P. (2000) *Trends Cell Biol.* **10,** 251–255
5. Söllner, T., Whitehart, S. W., Brunner, M., Erdjument-Bromage, H., Geromanos, S., Tempst, P., and Rothman, J. E. (1993) *Nature* **362,** 318–324
6. Søgaard, M., Tani, K., Ye, R. R., Geromanos, S., Tempst, P., Kirchhausen, T., Rothman, J. E., and Söllner, T. (1994) *Cell* **78,** 937–948
7. Götte, M., and Fischer von Mollard, G. (1998) *Trends Cell Biol.* **8,** 215–218
8. Hanson, P. I., Roth, R., Morisaki, H., Jahn, R., and Heuser, J. E. (1997) *Cell* **90,** 523–535
9. Sutton, R. B., Fasshauer, D., Jahn, R., and Brunger, A. T. (1998) *Nature* **395,** 347–353
10. Weber, T., Zemelman, B. V., Mcnew, J. A., Westermann, B., Gmachl, M., Parlati, F., Söllner, T. H., and Rothman, J. E. (1998) *Cell* **92,** 759–772
11. McNew, J. A., Parlati, F., Fukuda, R., Johnston, R. J., Paz, K., Paumet, F., Söllner, T. H., and Rothman, J. E. (2000) *Nature* **407,** 153–159
12. Yang, B., Gonzalez, L., Prekeris, R., Steegmaier, M., Advani, R. J., and Scheller, R. H. (1999) *J. Biol. Chem.* **274,** 5649–5653
13. Fasshauer, D., Antonin, W., Margittai, M., Pabst, S., and Jahn, R. (1999) *J. Biol. Chem.* **274,** 15440–15446
14. Nichols, B. J., and Pelham, H. R. (1998) *Biochim. Biophys. Acta* **1404,** 9–31
15. Götte, M., and Gallwitz, D. (1997) *FEBS Lett.* **411,** 48–52
16. Darsow, T., Rieder, S. E., and Emr, S. D. (1997) *J. Cell Biol.* **138,** 517–529
17. Grote, E., Vlacich, G., Pypaert, M., and Novick, P. J. (2000) *Mol. Biol. Cell* **11,** 4051–4065
18. Ballensiefen, W., Ossipov, D., and Schmitt, H. D. (1998) *J. Cell Sci.* **111,** 1507–1520
19. Ossipov, D., Schröder-Köhne, S., and Schmitt, H. D. (1999) *J. Cell Sci.* **112,** 4135–4142
20. Letourneur, F., Gaynor, E. C., Hennecke, S., Démollière, C., Duden, R., Emr, S. D., Riezman, H., and Cosson, P. (1994) *Cell* **79,** 1199–1207
21. Wieland, F., and Harter, C. (1999) *Curr. Opin. Cell Biol.* **11,** 440–446
22. Cosson, P., Démollière, C., Hennecke, S., Duden, R., and Letourneur, F. (1996) *EMBO J.* **15,** 1792–1798
23. Schröder-Köhne, S., Letourneur, F., and Riezman, H. (1998) *J. Cell Sci.* **111,** 3459–3470
24. Lewis, M. J., and Pelham, H. R. B. (1996) *Cell* **85,** 205–215
25. Todorow, Z., Spang, A., Carmack, E., Yates, J., and Schekman, R. (2000) *Proc. Natl. Acad. Sci. U. S. A.* **97,** 13643–13648
26. Dogic, D., Dubois, A., de Chassey, B., Lefkir, Y., and Letourneur, F. (2001) *Eur. J. Cell Biol.* **80,** 151–155
27. Dascher, C., Ossig, R., Gallwitz, D., and Schmitt, H. D. (1991) *Mol. Cell. Biol.* **11,** 872–885
28. Newman, A. P., Graf, J., Mancini, P., Rossi, G., Lian, J. P., and Ferro-Novick, S. (1992) *Mol. Cell. Biol.* **12,** 3663–3664

[3] U. Andag and H. D. Schmitt, unpublished observations.

29. Novick, P., Field, C., and Schekman, R. (1980) *Cell* **21,** 205–215
30. Lian, J. P., Stone, S., Jiang, Y., Lyons, P., and Ferro-Novick, S. (1994) *Nature* **372,** 698–701
31. Tsui, M. M., Tai, W. C., and Banfield, D. K. (2001) *Mol. Biol. Cell* **12,** 521–538
32. Lewis, M. J., Rayner, J. C., and Pelham, H. R. B. (1997) *EMBO J.* **16,** 3017–3024
33. Cosson, P., Schröder-Köhne, S., Sweet, D. S., Démollière, C., Hennecke, S., Frigerio, G., and Letourneur, F. (1997) *Eur. J. Cell Biol.* **73,** 93–97
34. Novick, P., Ferro, S., and Schekman, R. (1981) *Cell* **25,** 461–469
35. Newman, A. P., Shim, J., and Ferro-Novick, S. (1990) *Mol. Cell. Biol.* **10,** 3405–3414
36. Kaiser, C. A., and Schekman, R. (1990) *Cell* **61,** 723–733
37. Ossig, R., Dascher, C., Trepte, H. H., Schmitt, H. D., and Gallwitz, D. (1991) *Mol. Cell. Biol.* **11,** 2980–2993
38. Spang, A., and Schekman, R. (1998) *J. Cell Biol.* **143,** 589–599
39. Cao, X., and Barlowe, C. (2000) *J. Cell Biol.* **149,** 55–66
40. Fukuda, R., McNew, J. A., Weber, T., Parlati, F., Engel, T., Nickel, W., Rothman, J. E., and Söllner, T. H. (2000) *Nature* **407,** 198–202
41. Xu, D., Joglekar, A. P., Williams, A. L., and Hay, J. C. (2000) *J. Biol. Chem.* **275,** 39631–39639
42. Hatsuzawa, K., Hirose, H., Tani, K., Yamamoto, A., Scheller, R. H., and Tagaya, M. (2000) *J. Biol. Chem.* **275,** 13713–13720
43. VanRheenen, S. M., Reilly, B. A., Chamberlain, S. J., and Waters, M. G. (2001) *Traffic* **2,** 212–231
44. Elble, R. (1992) *BioTechniques* **13,** 18–20
45. Sherman, F., Fink, G. R., and Hicks, J. B. (1981) *Methods in Yeast Genetics*, Cold Spring Harbor Laboratory, Cold Spring Harbor, NY
46. Boehm, J., Letourneur, F., Ballensiefen, W., Ossipov, D., Démollière, C., and Schmitt, H. *D. (1997) J. Cell Sci.* **110,** 991–1003
47. De Antoni, A., and Gallwitz, D. (2000) *Gene* (*Amst.*) **246,** 179–185
48. Bender, A., and Pringle, J. R. (1991) *Mol. Cell. Biol.* **11,** 1295–1305
49. Orr-Weaver, T. L., Szostak, J. W., and Rothstein, R. J. (1981) *Proc. Natl. Acad. Sci. U. S. A.* **78,** 6354–6358
50. Evan, G. J., Lewis, G. K., Ramsay, G., and Bishop, J. M. (1985) *Mol. Cell. Biol.* 3610–3616
51. Schröder, S., Schimmöller, F., Singer-Krüger, B., and Riezman, H. (1995) *J. Cell Biol.* **131,** 895–912
52. Peng, R. W., Grabowski, R., DeAntoni, A., and Gallwitz, D. (1999) *Proc. Natl. Acad. Sci. U. S. A.* **96,** 3751–3756
53. Boehm, J., Ulrich, H. D., Ossig, R., and Schmitt, H. D. (1994) *EMBO J.* **13,** 3696–3710
54. Benli, M., Döring, F., Robinson, D. G., Yang, X., and Gallwitz, D. (1996) *EMBO J.* **15,** 6460–6475
55. Boecke, J. D., LaCroute, F., and Fink, G. R. (1984) *Mol. Gen. Genet.* **197,** 345–346
56. Entian, K. D., Schuster, T., Hegemann, J. H., Becher, D., Feldmann, H., Güldener, U., Götz, R., Hansen, M., Hollenberg, C. P., Jansen, G., Kramer, W., Klein, S., Kötter, P., Kricke, J., Launhardt, H., Mannhaupt, G., Maierl, A., Meyer, P., Mewes, W., Munder, T., Niedenthal, R. K., Ramezani Rad, M., Röhmer, A., Römer, A., and Hinnen, A. (1999) *Mol. Gen. Genet.* **262,** 683–702
57. Sapperstein, S. K., Lupashin, V. V., Schmitt, H. D., and Waters, M. G. (1996) *J. Cell Biol.* **132,** 755–767
58. VanRheenen, S. M., Cao, X. C., Lupashin, V. V., Barlowe, C., and Waters, M. G. (1998) *J. Cell Biol.* **141,** 1107–1119
59. VanRheenen, S. M., Cao, X., Sapperstein, S. K., Chiang, E. C., Lupashin, V. V., Barlowe, C., and Waters, M. G. (1999) *J. Cell Biol.* **147,** 729–742
60. Sacher, M., Jiang, Y., Barrowman, J., Scarpa, A., Burston, J., Zhang, L., Schieltz, D., Yates, J. R., Abeliovich, H., and Ferro-Novick, S. (1998) *EMBO J.* **17,** 2494–2503
61. McNew, J. A., Sogaard, M., Lampen, N. M., Machida, S., Ye, R. R., Lacomis, L., Tempst, P., Rothman, J. E., and Söllner, T. H. (1997) *J. Biol. Chem.* **272,** 17776–17783
62. Hicke, L., and Schekman, R. (1989) *EMBO J.* **8,** 1677–1684
63. Duden, R., Hosobuchi, M., Hamamoto, S., Winey, M., Byers, B., and Schekman, R. (1994) *J. Biol. Chem.* **269,** 24486–24495
64. Johnson, L. M., Bankaitis, V. A., and Emr, S. D. (1987) *Cell* **48,** 875–885
65. Semenza, J. C., Hardwick, K. G., Dean, N., and Pelham, H. R. B. (1990) *Cell* **61,** 1349–1357
66. Rose, M. D., Misra, L. M., and Vogel, J. P. (1989) *Cell* **57,** 1211–1221
67. Nishikawa, S., Hirata, A., and Nakano, A. (1994) *Mol. Biol. Cell* **5,** 1129–1143
68. Ito, T., Chiba, T., Ozawa, R., Yoshida, M., Hattori, M., and Sakaki, Y. (2001) *Proc. Natl. Acad. Sci. U. S. A.* **98,** 4569–4574
69. Hardwick, K. G., Boothroyd, J. C., Rudner, A. D., and Pelham, H. R. B. (1992) *EMBO J.* **11,** 4187–4195
70. Frigerio, G. (1998) *Yeast* **14,** 633–646
71. Simons, J. F., Ferro-Novick, S., Rose, M. D., and Helenius, A. (1995) *J. Cell Biol.* **130,** 41–49
72. Holst, B., Tachibana, C., and Winther, J. R. (1997) *J. Cell Biol.* **138,** 1229–1238
73. Sweet, D., and Pelham, H. R. B. (1993) *EMBO J.* **11,** 423–432

MEMBRANE TRANSPORT STRUCTURE FUNCTION AND BIOGENESIS:

The Coatomer-interacting Protein Dsl1p Is Required for Golgi-to-Endoplasmic Reticulum Retrieval in Yeast

Uwe Andag, Tanja Neumann and Hans Dieter Schmitt

J. Biol. Chem. 2001, 276:39150-39160.
doi: 10.1074/jbc.M105833200 originally published online August 7, 2001